Towards Real-World Document Parsing via Realistic Scene Synthesis and Document-Aware Training

Supplementary Material

1. Data Source

1.1. Document Element Sources

To construct a comprehensive element library for document parsing, we consolidate and utilize a variety of publicly available datasets across formulas, tables, and paragraphs. The detailed data sources are summarized in Table 1.

To enrich the diversity and generalization ability of our dataset, we conduct systematic data augmentation using the Qwen2.5-72B large language model (LLM). An overview of the augmentation pipeline is illustrated in Fig. 1. The augmentation procedures are tailored to the unique structure of each document element type and are described as follows:

Table Template Augmentation We perform table augmentation by modifying both content and layout structure:

- **Content Modification:** Table cell content is replaced with mathematical formulas or multilingual text corpora to increase linguistic and semantic diversity.
- **Structural Transformation:** Cells are randomly merged, split, or duplicated to generate novel table templates.

After augmentation, we apply rule-based post-processing to remove structurally invalid or semantically inconsistent tables. Final table-image and text-pair samples are synthesized using table rendering tools.

Formula Template Augmentation We augment LaTeX-formatted formulas by manipulating token sequences:

- **Symbol and Lexical Variation:** Symbols and word stems within formulas are systematically altered to increase symbolic diversity.
- **Structural Variation:** The spatial and logical composition of sub-formulas is reorganized to create new formula structures.

Invalid LaTeX expressions (e.g., non-compilable or syntactically incorrect) are filtered out. Valid formulas are rendered into isolated images using LaTeX rendering engines.

Paragraph-Level Data Augmentation We generate paragraph-level data with embedded formulas through two approaches:

- **Formula-Text Fusion:** Generated LaTeX formulas are inserted into natural language paragraphs, which are then rendered to create image-text pairs that simulate real-world academic content.
- **Semantic Paragraph Synthesis:** The LLM is used to generate semantically coherent multi-paragraph text blocks, which are rendered as full-page document images. The corresponding text corpus is preserved for further alignment and downstream synthesis tasks.
- **Multilingual Data Augmentation:** To enhance cross-lingual document understanding, we employ LLM-based translation to convert corpora into multiple languages, thereby enriching the dataset with a diverse set of multilingual samples.

This hierarchical augmentation pipeline ensures a high degree of variability and realism across multiple document modalities, forming a robust foundation for document analysis and understanding. In total, we consolidate both the original and augmented data, resulting in a unified corpus comprising 3.1 million table instances, 3.3 million formula samples, and 3 million paragraph-level documents.

1.2. Layout Sources

Our layout templates are primarily derived from three sources to ensure both structural diversity and annotation consistency.

1) Public Benchmarks We curate a set of publicly available layout datasets[7, 17, 27] that provide reading order annotations. These datasets serve as the foundation of our layout template library. To address inconsistencies in annotation schemas, we normalize all category labels to a unified taxonomy, reducing ambiguity across datasets. For each document, we extract structured layout information, including the original image dimensions and the bounding box coordinates of each layout element. These data points are recorded as digital layout templates.

2) High-Confidence Model Inference To further enrich our layout template diversity, we apply a pre-trained layout analysis model to a set of structured documents. Inference results with high confidence scores and minimal inter-region overlap are retained. This filtering ensures the structural integrity of the layout while augmenting the dataset with additional real-world layout variations.

3) Composite Layout Construction To simulate dense layout scenarios found in newspapers and book pages, we further construct composite templates by concatenating multiple single-page layouts into unified multi-section

Table 1. Document element datasets and corresponding formats.

Element Type	Datasets	Format
Table Parsing	FinTabNet [20], PubTabNet [30], TalTabNet [5]	HTML
Formula Parsing	UniMER [21], CROHME14 [12], CROHME16 [13], CROHME19 [10], HME [26]	LaTeX
Paragraph Parsing	FOX [9], GOT [24]	Text

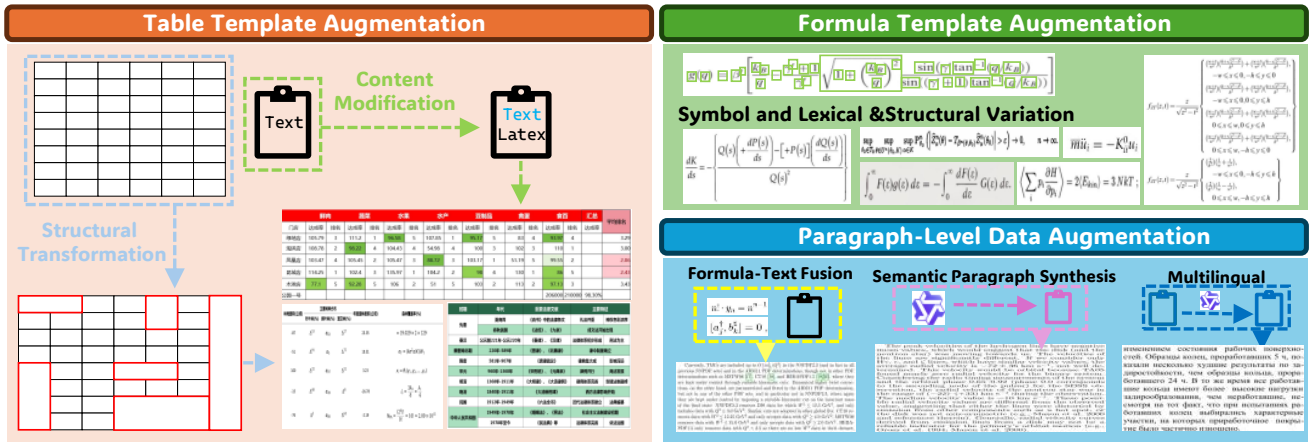

Figure 1. **Element-Aware Augmentation Pipeline.** Qwen2.5-72B drives content- and structure-level edits for tables, formulas, and paragraphs, followed by rule-based validation and LaTeX rendering to produce image–annotation pairs.

documents. To preserve rendering quality and visual coherence, we constrain the number of merged layout modules to a maximum of 50 per composite document.

By combining curated benchmarks with reliable model-generated samples, we construct a robust and diverse layout template corpus for downstream layout-aware tasks.

2. Supplementary Experiments

2.1. Sub-element Parsing Evaluation

To evaluate DocHumming's effectiveness on fine-grained document understanding tasks, we conduct a series of benchmarking experiments on sub-element parsing. Our model is compared against both specialized open-source methods and widely used commercial APIs across multiple public datasets.

2.1.1. Mathematical Formula Recognition.

Handwritten setting. We first evaluate handwritten formula recognition on **HME100K** [26] and **CROHME** [10, 12, 13], reporting *Expression Recognition Rate* (ExpRate) and *Character Deletion Metric* (CDM) [22]; results are summarized in Table 2. We also assess cross-domain robustness on **UniMER** [21], with results in Table 3. *DocHumming* improves HME ExpRate by **8.72%** and surpasses state-of-the-art methods across CROHME editions, while maintaining strong generalization on UniMER (printed/handwritten, syntactic/semantic variants), which we attribute to instruction-tuned pretraining and structure-aware optimization.

Digital/scanned setting. To measure formula parsing on typeset documents, we further evaluate the *Formula-Block* subset of **OmniDocBench** (scanned/digital) [15]. Results in Table 4 (CDM↑) show that *DocHumming* reaches a CDM of **0.9741**, outperforming strong modular and end-to-end baselines; it yields a **+2.88** point absolute gain over the best prior system. These results indicate that our unified training recipe and realistic synthesis not only benefit handwritten formulas but also deliver state-of-the-art accuracy on clean typeset pages.

Table 2. Performance comparison on **CROHME** and **HME** datasets for mathematical formula recognition.

Dataset	Method	ExpRate	≤ 1	≤ 2	≤ 3
CROHME 14 [12]	PosFormer [4]	62.74	78.47	84.16	88.32
	DocHumming	**70.48**	**81.54**	**86.91**	**90.16**
CROHME 16 [13]	PosFormer	61.02	77.07	83.60	88.14
	DocHumming	**67.56**	**82.04**	**89.27**	**92.15**
CROHME 19 [10]	PosFormer	64.97	81.23	85.48	88.15
	DocHumming	**68.39**	**82.98**	**88.24**	**91.24**
HME [26]	PosFormer	69.06	84.58	89.94	92.45
	DocHumming	**77.78**	**89.77**	**93.49**	**95.15**

Table 3. Performance comparison on the **UniMER** benchmark for mathematical formula recognition.

Method	SPE	CPE	HWE	SCE
	CDM↑	CDM↑	CDM↑	CDM↑
Pix2tex [2]	96.19	64.89	24.53	67.62
Texify [16]	98.52	70.41	52.69	79.32
Mathpix [11]	97.29	**96.71**	93.18	92.38
UniMERNet [21]	**99.14**	95.95	94.00	93.73
DocHumming	98.91	96.61	**96.85**	**94.91**

Table 4. Results on **OmniDocBench–Formula-Block** (CDM↑). Best in **bold**, second best underlined.

Method	CDM↑
dots.ocr [18]	0.4641
MinerU2-VLM [23]	0.8286
MonkeyOCR-pro-1.2B [8]	0.8531
MonkeyOCR-3B [8]	0.8621
Qwen2.5-VL-72B [1]	0.8747
MinerU2.5 [14]	0.9187
PaddleOCR-VL [3]	0.9453
DocHumming (Ours)	**0.9741**

2.1.2. End-to-End Table Parsing

We evaluate end-to-end table parsing on FinTabNet [28] and PubTabNet [29], employing TEDS and TEDS-S as structural and semantic evaluation metrics, and the experimental results are presented in Table 5.

Our model achieves superior performance in table parsing tasks, outperforming OmniParser V2 [25] by **5.4%** on FinTabNet and **6.5%** on PubTabNet in Structure-TEDS. When incorporating text into evaluation, DocHumming exhibits even greater improvements, outperforming OmniParser V2 by **7.6%** on FinTabNet and **7.1%** on PubTabNet.

Table 5. Performance comparison on FinTabNet and PubTabNet benchmarks for end-to-end table parsing.

Method	FinTabNet		PubTabNet	
	S-TEDS↑	TEDS↑	S-TEDS↑	TEDS↑
Donut [6]	30.6	29.1	25.2	22.7
EDD [31]	90.6	–	89.9	88.3
OmniParser V2 [25]	93.2	90.5	90.5	88.9
DocHumming	**98.6**	**98.1**	**97.0**	**96.0**

OmniDocBench-Table-block. We further test cropped-table parsing on **OmniDocBench-Table-block**. *DocHumming* attains **0.9421 TEDS** and **0.9693 Structural TEDS**, outperforming strong modular and E2E baselines. *DocHumming* improves over the best baseline (PaddleOCR-VL) by **+2.26** TEDS and **+1.50** Structural TEDS, confirming strong structural fidelity on real printed layouts.

Table 6. Results on OmniDocBench-Table-block (cropped tables).

Method	Overall TEDS↑	Structural TEDS↑
MinerU2-VLM [23]	0.9002	0.9369
Seed1.6 [19]	0.9079	0.9489
dots.ocr [18]	0.8194	0.8442
MinerU2.5 [14]	0.9005	0.9539
PaddleOCR-VL [3]	0.9195	0.9543
DocHumming	**0.9421**	**0.9693**

2.2. Effect of Structural Loss Weight λ

To evaluate the impact of structural supervision, we conduct an ablation study on the structural loss weight λ, which balances the contribution of structure-aware loss during training. The results across various λ settings are presented in Table 7, based on the OmniDocBench benchmark.

Table 7. Impact of structural loss weight λ on OmniDocBench performance and redundancy rate.

#	OmniDocBench	
	Overall	Repeat (%)
$\lambda = 1$	88.74	4.6
$\lambda = 2$	92.81	3.4
$\lambda = 4$	**93.75**	**2.1**
$\lambda = 6$	93.60	2.1

As shown in Table 7, increasing λ consistently reduces the repeat rate, indicating that structural guidance helps mitigate output redundancy. This improvement is attributed to breaking the uniform treatment of tokens in autoregressive decoding by introducing stronger structure-aware optimization.

However, when λ becomes too large (e.g., 6), we observe a slight degradation in performance despite the stable repeat rate. This suggests an overemphasis on structure-dominated samples during training, which leads to suboptimal balance across other element types and table elements.

Our results suggest that setting $\lambda = 4$ offers the best trade-off between structured accuracy and generation coherence.

3. DocMix Visualization

To help better illustrate the annotation schema and overall data quality of the DocMix dataset, we provide a set of representative samples as part of the supplementary materials. These examples are intended to support a deeper under-

standing of the document parsing rules adopted in DocMix and the variety of content types included in the dataset.

4. Wild-OmniDocBench Visualization

We additionally include a small set of Wild-OmniDocBench examples in the supplementary package. Image filenames are exactly aligned with the original OmniDocBench images, so users can directly cross-reference the official OmniDocBench annotations for label alignment.

5. Test Case Analysis

To further demonstrate the robustness and adaptability of DocHumming in diverse real-world scenarios, we supplement our evaluation with test cases collected from various web-sourced document images. These additional samples cover a wide range of formats and layouts beyond the original training distribution.

We visualize several representative parsing results in Figs. 2 and 3. These examples highlight DocHumming's ability to handle noisy inputs and uncommon layout structures, reflecting its strong generalization capabilities across domains.

6. Error Case Analysis

We conduct an error analysis on web-scraped document images by running *DocHumming* inference and selecting cases whose outputs (i) hit the maximum output length (8,192 tokens) and (ii) exhibit repetitive decoding. We categorize the failures into four major types (see Fig. 4 for examples):

- **Ultra–high-resolution pages.** Very large pages require downsampling or tiling, which can trigger repeated or missing content in dense regions.
- **Irregular, interleaved layouts.** Non-standard pages (e.g., interwoven/nested blocks in newspapers or posters) blur structural boundaries and reading order.
- **Oversized structured tables.** Long tables with many rows/columns magnify exposure bias and increase repetition near structural delimiters.
- **Extreme aspect ratios.** Very tall or wide images reduce effective resolution for fine details and destabilize long-context decoding.

These observations suggest targeted improvements on both axes: **model**—enhanced layout-aware perception for irregular structures, resolution-adaptive processing for ultra–large pages with cross-tile consistency, and more stable long-context decoding; **data**—augment *Realistic Scene Synthesis* with page-level content that emphasizes semantic consistency and logical coherence across elements, plus dedicated stress tests for extreme sizes and aspect ratios. Representative failure cases and visualizations are provided in Fig. 4.

References

[1] Shuai Bai, Keqin Chen, Xuejing Liu, Jialin Wang, Wenbin Ge, Sibo Song, Kai Dang, Peng Wang, Shijie Wang, Jun Tang, Humen Zhong, Yuanzhi Zhu, Mingkun Yang, Zhaohai Li, Jianqiang Wan, Pengfei Wang, Wei Ding, Zheren Fu, Yiheng Xu, Jiabo Ye, Xi Zhang, Tianbao Xie, Zesen Cheng, Hang Zhang, Zhibo Yang, Haiyang Xu, and Junyang Lin. Qwen2.5-vl technical report. *arXiv preprint arXiv:2502.13923*, 2025. 3

[2] BreezeDeus. Pix2text: Image-to-latex ocr tool. https://github.com/breezedeus/Pix2Text, 2024. Accessed: 2025-07-30. 3

[3] Cheng Cui, Ting Sun, Suyin Liang, Tingquan Gao, Zelun Zhang, Jiaxuan Liu, Xueqing Wang, Changda Zhou, Hongen Liu, Manhui Lin, et al. Paddleocr-vl: Boosting multilingual document parsing via a 0.9 b ultra-compact vision-language model. *arXiv preprint arXiv:2510.14528*, 2025. 3

[4] Tongkun Guan, Chengyu Lin, Wei Shen, and Xiaokang Yang. Posformer: Recognizing complex handwritten mathematical expression with position forest transformer. *arXiv preprint arXiv:2407.07764*, 2024. 2

[5] Heywhale. taltab. https://www.heywhale.com/home/competition/606d6fff0e04ac0017c3bf7f/content/1, 2021. Accessed: 2025-08-02. 2

[6] Geewook Kim, Teakgyu Hong, Moonbin Yim, JeongYeon Nam, Jinyoung Park, Jinyeong Yim, Wonseok Hwang, Sangdoo Yun, Dongyoon Han, and Seunghyun Park. Ocr-free document understanding transformer. In *European Conference on Computer Vision (ECCV)*, 2022. 3

[7] Lihang Li. Cdla: A comprehensive dataset for layout-aware document understanding. https://github.com/buptlihang/CDLA, 2024. Accessed: 2025-07-28. 1

[8] Zhang Li, Yuliang Liu, Qiang Liu, Zhiyin Ma, Ziyang Zhang, Shuo Zhang, Zidun Guo, Jiarui Zhang, Xinyu Wang, and Xiang Bai. Monkeyocr: Document parsing with a structure-recognition-relation triplet paradigm. *arXiv preprint arXiv:2506.05218*, 2025. 3

[9] Chenglong Liu, Haoran Wei, Jinyue Chen, Lingyu Kong, Zheng Ge, Zining Zhu, Liang Zhao, Jianjian Sun, Chunrui Han, and Xiangyu Zhang. Focus anywhere for fine-grained multi-page document understanding. *arXiv preprint arXiv:2405.14295*, 2024. 2

[10] Mahshad Mahdavi, Richard Zanibbi, Harold Mouchere, Christian Viard-Gaudin, and Utpal Garain. Icdar 2019 crohme+ tfd: Competition on recognition of handwritten mathematical expressions and typeset formula detection. In *2019 International Conference on Document Analysis and Recognition (ICDAR)*, pages 1533–1538. IEEE, 2019. 2

[11] Mathpix. Mathpix Snip: Convert images and PDFs to LaTeX, DOCX, and more. https://mathpix.com/, 2025. 3

[12] Harold Mouchere, Christian Viard-Gaudin, Richard Zanibbi, and Utpal Garain. Icfhr 2014 competition on recognition of on-line handwritten mathematical expressions (crohme

2014). In *2014 14th International Conference on Frontiers in Handwriting Recognition*, pages 791–796. IEEE, 2014. 2

[13] Harold Mouchère, Christian Viard-Gaudin, Richard Zanibbi, and Utpal Garain. Icfhr2016 crohme: Competition on recognition of online handwritten mathematical expressions. In *2016 15th International Conference on Frontiers in Handwriting Recognition (ICFHR)*, pages 607–612. IEEE, 2016. 2

[14] Junbo Niu, Zheng Liu, Zhuangcheng Gu, et al. Mineru2.5: A decoupled vision-language model for efficient high-resolution document parsing, 2025. 3

[15] Linke Ouyang, Yuan Qu, Hongbin Zhou, Jiawei Zhu, Rui Zhang, Qunshu Lin, Bin Wang, Zhiyuan Zhao, Man Jiang, Xiaomeng Zhao, Jin Shi, Fan Wu, Pei Chu, Minghao Liu, Zhenxiang Li, Chao Xu, Bo Zhang, Botian Shi, Zhongying Tu, and Conghui He. Omnidocbench: Benchmarking diverse pdf document parsing with comprehensive annotations, 2024. 2

[16] Vik Paruchuri. Texify: Turn images into latex. https://github.com/VikParuchuri/texify, 2022. Accessed: 2025-08-01. 3

[17] Birgit Pfitzmann, Christoph Auer, Michele Dolfi, Ahmed S Nassar, and Peter W J Staar. Doclaynet: A large human-annotated dataset for document-layout analysis. 2022. 1

[18] rednote hilab. dots.ocr, 2025. 3

[19] Seed. Seed1.6, 2025. 3

[20] Brian Smock. Fintabnet.c: Financial table recognition dataset. https://huggingface.co/datasets/bsmock/FinTabNet.c, 2024. Accessed: 2025-08-02. 2

[21] Bin Wang, Zhuangcheng Gu, Guang Liang, Chao Xu, Bo Zhang, Botian Shi, and Conghui He. Unimernet: A universal network for real-world mathematical expression recognition. *arXiv preprint arXiv:2404.15254*, 2024. 2, 3

[22] Bin Wang, Fan Wu, Linke Ouyang, Zhuangcheng Gu, Rui Zhang, Renqiu Xia, Bo Zhang, and Conghui He. Cdm: A reliable metric for fair and accurate formula recognition evaluation. *arXiv preprint arXiv:2409.03643*, 2024. 2

[23] Bin Wang, Chao Xu, Xiaomeng Zhao, Linke Ouyang, Fan Wu, Zhiyuan Zhao, Rui Xu, Kaiwen Liu, Yuan Qu, Fukai Shang, Bo Zhang, Liqun Wei, Zhihao Sui, Wei Li, Botian Shi, Yu Qiao, Dahua Lin, and Conghui He. Mineru: An open-source solution for precise document content extraction, 2024. 3

[24] Haoran Wei, Chenglong Liu, Jinyue Chen, Jia Wang, Lingyu Kong, Yanming Xu, Zheng Ge, Liang Zhao, Jianjian Sun, Yuang Peng, et al. General ocr theory: Towards ocr-2.0 via a unified end-to-end model. *arXiv preprint arXiv:2409.01704*, 2024. 2

[25] Wenwen Yu, Zhibo Yang, Jianqiang Wan, Sibo Song, Jun Tang, Wenqing Cheng, Yuliang Liu, and Xiang Bai. Omniparser v2: Structured-points-of-thought for unified visual text parsing and its generality to multimodal large language models. *arXiv preprint arXiv:2502.16161*, 2025. 3

[26] Ye Yuan, Xiao Liu, Wondimu Dikubab, Hui Liu, Zhilong Ji, Zhongqin Wu, and Xiang Bai. Syntax-aware network for handwritten mathematical expression recognition. *arXiv preprint arXiv:2203.01601*, 2022. 2

[27] Zhiyuan Zhao, Hengrui Kang, Bin Wang, and Conghui He. Doclayout-yolo: Enhancing document layout analysis through diverse synthetic data and global-to-local adaptive perception, 2024. 1

[28] Xinyi Zheng, Doug Burdick, Lucian Popa, Peter Zhong, and Nancy Xin Ru Wang. Global table extractor (gte): A framework for joint table identification and cell structure recognition using visual context. *Winter Conference for Applications in Computer Vision (WACV)*, 2021. 3

[29] Xu Zhong, Elaheh ShafieiBavani, and Antonio Jimeno Yepes. Image-based table recognition: data, model, and evaluation. *arXiv preprint arXiv:1911.10683*, 2019. 3

[30] Xingjian Zhong, Jialong Han, Chao Xu, and Caiming Xiong. Pubtabnet: Image-to-table generation using multimodal learning. https://github.com/ibm-aur-nlp/PubTabNet, 2020. Accessed: 2025-08-02. 2

[31] Xu Zhong, Elaheh ShafieiBavani, and Antonio Jimeno Yepes. Image-based table recognition: data, model, and evaluation. In *European conference on computer vision*, pages 564–580. Springer, 2020. 3

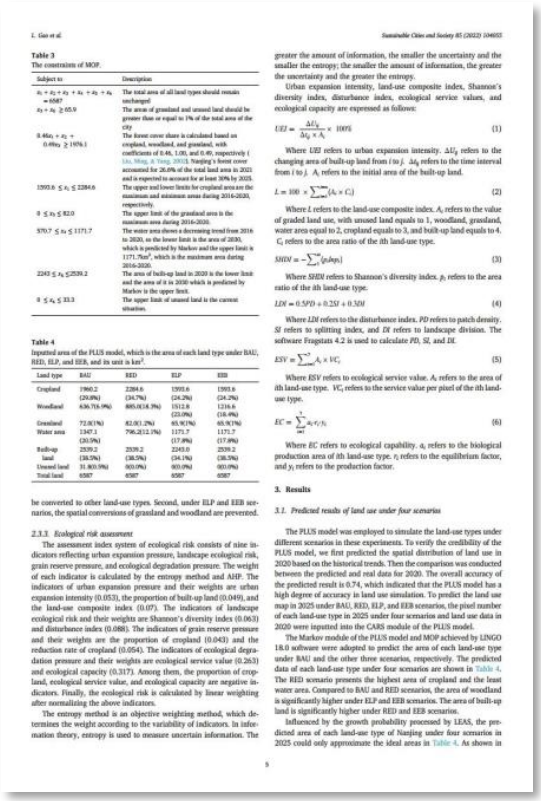

L. Gao et al. Sustainable Cities and Society 85 (2022) 104055

greater the amount of information, the smaller the uncertainty and the smaller the entropy; the smaller the amount of information, the greater the uncertainty and the greater the entropy.

Urban expansion intensity, land-use composite index, Shannon's diversity index, disturbance index, ecological service values, and ecological capacity are expressed as follows:

$$UEI = \frac{\Delta U_{ij}}{\Delta t_{ij} \times A_i} \times 100\% \quad (1)$$

Where UEI refers to urban expansion intensity. ΔU_{ij} refers to the changing area of built-up land from i to j. Δt_{ij} refers to the time interval from i to j. A_i refers to the initial area of the built-up land.

$$L = 100 \times \sum_{i=1}^{n} (A_i \times C_i) \quad (2)$$

Where L refers to the land-use composite index. A_i refers to the value of graded land use, with unused land equals to 1, woodland, grassland, water area equal to 2, cropland equals to 3, and built-up land equals to 4. C_i refers to the area ratio of the ith land-use type.

$$SHDI = -\sum_{i=1}^{m} (p_i \ln p_i) \quad (3)$$

Where $SHDI$ refers to Shannon's diversity index. p_i refers to the area ratio of the ith land-use type.

$$LDI = 0.5PD + 0.2SI + 0.3DI \quad (4)$$

Where LDI refers to the disturbance index. PD refers to patch density. SI refers to splitting index, and DI refers to landscape division. The software Fragstats 4.2 is used to calculate PD, SI, and DI.

$$ESV = \sum_{i=1}^{n} A_i \times VC_i \quad (5)$$

Where ESV refers to ecological service value. A_i refers to the area of ith land-use type. VC_i refers to the service value per pixel of the ith land-use type.

$$EC = \sum_{i=1}^{n} a_i \times r_i \times y_i \quad (6)$$

Where EC refers to ecological capability. a_i refers to the biological production area of ith land-use type. r_i refers to the equilibrium factor, and y_i refers to the production factor.

3. Results

3.1. Predicted results of land use under four scenarios

The PLUS model was employed to simulate the land-use types under different scenarios in these experiments. To verify the credibility of the PLUS model, we first predicted the spatial distribution of land use in 2020 based on the historical trends. Then the comparison was conducted between the predicted and real data for 2020. The overall accuracy of the predicted result is 0.74, which indicated that the PLUS model has a high degree of accuracy in land use simulation. To predict the land use map in 2025 under BAU, RED, ELP, and EEB scenarios, the pixel number of each land-use type in 2025 under four scenarios and land use data in 2020 were inputted into the CARS module of the PLUS model.

The Markov module of the PLUS model and MOP achieved by LINGO 18.0 software were adopted to predict the area of each land-use type under BAU and the other three scenarios, respectively. The predicted data of each land-use type under four scenarios are shown in Table 4. The RED scenario presents the highest area of cropland and the least water area. Compared to BAU and RED scenarios, the area of woodland is significantly higher under ELP and EEB scenarios. The area of built-up land is significantly higher under RED and EEB scenarios.

Influenced by the growth probability processed by LEAS, the predicted area of each land-use type of Nanjing under four scenarios in 2025 could only approximate the ideal areas in Table 4. As shown in

Table 3
The constraints of MOP.

Subject to	Description
$x_1 + x_2 + x_3 + x_4 + x_5 + x_6 = 6587$	The total area of all land types should remain unchanged
$x_3 + x_6 \geq 65.9$	The area of grassland and unused land should be greater than or equal to 1% of the total area of the city
$0.46x_1 + x_2 + 0.69x_3 \geq 1976.1$	The forest cover share is calculated based on cropland, woodland, and grassland, with coefficients of 0.46, 1.00, and 0.69, respectively (Liu, Ming, & Yang, 2002). Nanjing's forest cover accounted for 26.6% of the total land area in 2021 and is expected to account for at least 30% by 2025.
$1593.6 \leq x_1 \leq 2284.6$	The upper and lower limits for cropland area are the maximum and minimum areas during 2016-2020, respectively.
$0 \leq x_2 \leq 82.0$	The upper limit of the grassland area is the maximum area during 2016-2020.
$570.7 \leq x_4 \leq 1171.7$	The water area shows a decreasing trend from 2016 to 2020, so the lower limit is the area of 2020, which is predicted by Markov and the upper limit is $1171.75 km^2$ (2), which is the maximum area during 2016-2020.
$2243 \leq x_5 \leq 2539.2$	The area of built-up land in 2020 is the lower limit and the area of it in 2030 which is predicted by Markov is the upper limit.
$0 \leq x_6 \leq 33.3$	The upper limit of unused land is the current situation.

Table 4
Inputted area of the PLUS model, which is the area of each land type under BAU, RED, ELP, and EEB, and its unit is km^2.

Land type	BAU	RED	ELP	EEB
Cropland	1960.2 (29.8%)	2284.6 (34.7%)	1593.6 (24.2%)	1593.6 (24.2%)
Woodland	636.7(9.7%)	805.0(12.3%)	1512.8 (23.0%)	1216.6 (18.4%)
Grassland	72.0(1%)	82.0(1.2%)	65.9(1%)	65.9(1%)
Water area	1347.1 (20.5%)	796.2(12.1%)	1171.7 (17.8%)	1171.7 (17.8%)
Built-up land	2539.2 (38.5%)	2539.2 (38.5%)	2243.0 (34.1%)	2539.2 (38.5%)
Unused land	31.8(0.5%)	0(0.0%)	0(0.0%)	0(0.0%)
Total land	6587	6587	6587	6587

be converted to other land-use types. Second, under ELP and EEB scenarios, the spatial conversions of grassland and woodland are prevented.

2.3.3. Ecological risk assessment

The assessment index system of ecological risk consists of nine indicators reflecting urban expansion pressure, landscape ecological risk, grain reserve pressure, and ecological degradation pressure. The weight of each indicator is calculated by the entropy method and AHP. The indicators of urban expansion pressure and their weights are urban expansion intensity (0.053), the proportion of built-up land (0.049), and the land-use composite index (0.07). The indicators of landscape ecological risk and their weights are Shannon's diversity index (0.063) and disturbance index (0.088). The indicators of grain reserve pressure and their weights are the proportion of cropland (0.043) and the reduction rate of cropland (0.054). The indicators of ecological degradation pressure and their weights are ecological service value (0.263) and ecological capacity (0.317). Among them, the proportion of cropland, ecological service value, and ecological capacity are negative indicators. Finally, the ecological risk is calculated by linear weighting after normalizing the above indicators.

The entropy method is an objective weighting method, which determines the weight according to the variability of indicators. In information theory, entropy is used to measure uncertain information. The

Table 3
the constraints of MOP

Subject to	Description
$ x_{1} + x_{2} + x_{3} + x_{4} + x_{5} + x_{6} = 6587 $	the total area of all land types should remain unchanged
$ x_{3} + x_{6} \geq 65.9 $	the area of grassland and unused land should be greater than or equal to 1% of the total area of the city
$ 0.46x_{1} + x_{2} + 0.69x_{3} \geq 1976.1 $	the forest cover share is calculated based on cropland, woodland, and grassland, with coefficients of 0.46, 1.00, and 0.69, respectively (Liu, Ming, & Yang, 2002). Nanjing's forest accounted for 26.6% of the total land area in 2021 and is expected to account for at least 30% by 2025.
$ 1593.6 \leq x_{1} \leq 2284.6 $	the upper and lower limits for cropland area are the maximum and minimum areas during 2016 - 2020, respectively.
$ 0 \leq x_{2} \leq 82.0 $	the upper limit of the grassland area is the maximum area during 2016 - 2020.
$ 570.7 \leq x_{4} \leq 1171.7 $	the water area shows a decreasing trend from 2016 to 2020, so the lower limit is the area of 2030, which is predicted by Markov and the upper limit is 1171.75 km^{2} (2) $, which is the maximum area during 2016 - 2020.
$ 2243 \leq x_{5} \leq 2539.2 $	the area of built - up land in 2020 is the lower limit and the area of it in 2030 which is predicted by Markov is the upper limit.
$ 0 \leq x_{6} \leq 33.3 $	the upper limit of unused land is the current situation.

PGI=0.66.

Table 4
Inputted area of the PLUS model, which is the area of each land type under BAU, RED, ELP, and EEB, and its unit is $ km^{2} $.

Land type	BAU	RED	ELP	EEB
Cropland	1960.2 (29.8%)	2284.6 (34.7%)	1593.6 (24.2%)	1593.6 (24.2%)
Woodland	636.7(8.9%)	805.0(10.3%)	1512.8 (23.0%)	1216.6 (18.4%)
Grassland	72.0(1%)	82.0(1.2%)	65.9(1%)	65.9(1%)
Water area	1347.1 (20.5%)	796.2(12.1%)	1171.7 (17.8%)	1171.7 (17.8%)
Built - up land	2539.2 (38.5%)	2539.2 (38.5%)	2243.0 (34.1%)	2539.2 (38.5%)
Unused land	31.8(0.5%)	0(0.0%)	0(0.0%)	0(0.0%)
Total land	6587	6587	6587	6587

be converted to other land - use types. Second, under ELP and EEB sce - narios, the spatial conversions of grassland and woodland are prevented.

2.3.3. Ecological risk assessment

The assessment index system of ecological risk consists of nine in - dicators reflecting urban expansion pressure, landscape ecological risk, grain reserve pressure, and ecological degradation pressure. The weight of each indicator is calculated by the entropy method and AHP. The indicators of urban expansion pressure and their weights are urban expansion intensity (0.053), the proportion of built - up land (0.049), and the land - use composite index (0.07). The indicators of landscape ecological risk and their weights are Shannon's diversity index (0.063) and disturbance index (0.088). The indicators of grain reserve pressure and their weights are the proportion of cropland (0.043) and the reduction rate of cropland (0.054). The indicators of ecological degra - dation pressure and their weights are ecological service value (0.263) and ecological capacity (0.317). Among them, the proportion of crop - land, ecological service value, and ecological capacity are negative in - dicators. Finally, the ecological risk is calculated by linear weighting after normalizing the above indicators.

The entropy method is an objective weighting method, which de - termines the weight according to the variability of indicators. In infor - mation theory, entropy is used to measure uncertain information. The greater the amount of information, the smaller the uncertainty and the smaller the entropy; the smaller the amount of information, the greater the uncertainty and the greater the entropy.

Urban expansion intensity, land - use composite index, Shannon's diversity index, disturbance index, ecological service values, and ecological capacity are expressed as follows:

$$ UEI=\frac{\Delta U_{ij}}{\Delta t_{ij}\times A_{i}}\times 100\% \qquad(1) $$

Where UEI refers to urban expansion intensity. $ \Delta U_{ij} $ refers to the changing area of built - up land from i to j. $ \Delta t_{ij} $ refers to the time interval from i to j. $ A_{i} $ refers to the initial area of the built - up land.

$$ L = 100\times\sum\limits_{i=1}^{n}(A_{i}\times C_{i}) \qquad(2) $$

Where L refers to the land - use composite index. $ A_{i} $ refers to the value of graded land use, with unused land equals to 1, woodland, grassland, water area equal to 2, cropland equals to 3, and built - up land equals to 4. $ C_{i} $ refers to the area ratio of the ith land - use type.

$$ SHDI=-\sum\limits_{i=1}^{m}(p_{i}\ln p_{i}) \qquad(3) $$

Where SHDI refers to Shannon's diversity index. $ p_{i} $ refers to the area ratio of the i th land - use type.

$$ LDI = 0.5PD+0.2SI+0.3DI \qquad(4) $$

Where LDI refers to the disturbance index. PD refers to patch density. SI refers to splitting index, and DI refers to landscape division. The software Fragstats 4.2 is used to calculate PD, SI, and DI.

$$ ESV=\sum\limits_{i=1}^{n}A_{i}\times VC_{i} \qquad(5) $$

Where ESV refers to ecological service value. $ A_{i} $ refers to the area of i th land - use type. $ VC_{i} $ refers to the service value per pixel of the i th land - use type.

$$ EC=\sum\limits_{i=1}^{n}a_{i}\times r_{i}\times y_{i} \qquad(6) $$
Where EC refers to ecological capability. $ a_{i} $ refers to the biological production area of i th land - use type. $ r_{i} $ refers to the equilibrium factor, and $ y_{i} $ refers to the production factor.

3. Results

3.1. Predicted results of land use under four scenarios

The PLUS model was employed to simulate the land - use types under different scenarios in these experiments. To verify the credibility of the PLUS model, we first predicted the spatial distribution of land use in 2020 based on the historical trends. Then the comparison was conducted between the predicted and real data for 2020. The overall accuracy of the predicted result is 0.74, which indicated that the PLUS model has a high degree of accuracy in land use simulation. To predict the land use map in 2025 under BAU, RED, ELP, and EEB scenarios, the pixel number of each land - use type in 2025 under four scenarios and land use data in 2020 were inputted into the CARS module of the PLUS model.

The Markov module of the PLUS model and MOP achieved by LINGO 18.0 software were adopted to predict the area of each land - use type under BAU and the other three scenarios, respectively. The predicted data of each land - use type under four scenarios are shown in Table 4.The RED scenario presents the highest area of cropland and the least water area. Compared with BAU and RED scenarios, the area of woodland is significantly higher under ELP and EEB scenarios. The area of built - up land is significantly higher under RED and EEB scenarios.

Influenced by the growth probability processed by LEAS, the pre - dicted area of each land - use type of Nanjing under four scenarios in 2025 could only approximate the ideal areas in Table 4. As shown in

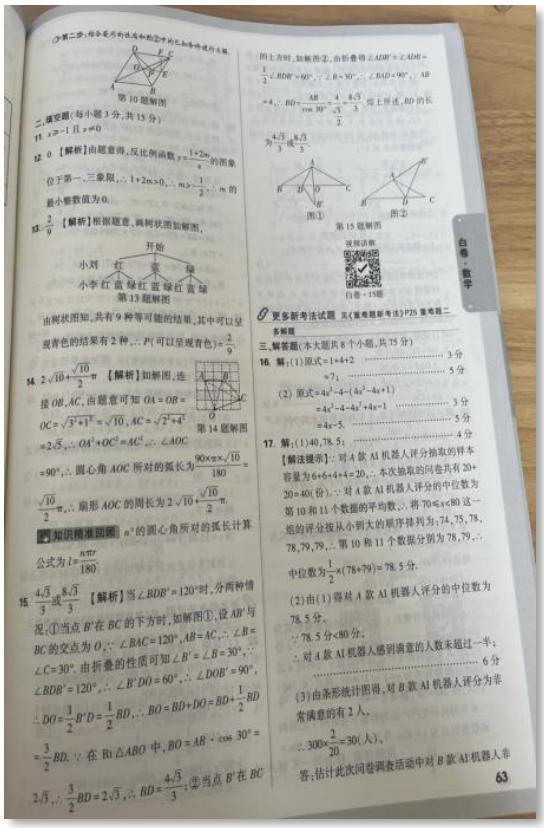

第 10 题解图

二、填空题(每小题 3 分,共 15 分)

11. $x\geqslant -1$ 且 $x\neq 0$

12. 0 【解析】由题意得,反比例函数 $y=\frac{1+2m}{x}$ 的图象位于第一、三象限,$\therefore 1+2m>0$,$\therefore m>-\frac{1}{2}$,$\therefore$ m 的最小整数值为 0.

13. $\frac{2}{9}$ 【解析】根据题意,画树状图如解图.

第 13 题解图

由树状图知,共有 9 种等可能的结果,其中可以呈现青色的结果有 2 种,$\therefore P$(可以呈现青色)$=\frac{2}{9}$.

14. $2\sqrt{10}+\frac{\sqrt{10}}{2}\pi$ 【解析】如解图,连接 OB,AC,由题意可知 $OA=OB=OC=\sqrt{3^2+1^2}=\sqrt{10}$,$AC=\sqrt{2^2+4^2}=2\sqrt{5}$,$\therefore OA^2+OC^2=AC^2$,$\therefore \angle AOC=90^\circ$,$\therefore$ 圆心角 AOC 所对的弧长为 $\frac{90\times\pi\times\sqrt{10}}{180}=\frac{\sqrt{10}}{2}\pi$,$\therefore$ 扇形 AOC 的周长为 $2\sqrt{10}+\frac{\sqrt{10}}{2}\pi$.

第 14 题解图

知识精准回顾 n°的圆心角所对的弧长计算公式为 $l=\frac{n\pi r}{180}$.

15. $\frac{4\sqrt{3}}{3}$或$\frac{8\sqrt{3}}{3}$ 【解析】当 $\angle BDB'=120^\circ$ 时,分两种情况:①当点 B' 在 BC 的下方时,如解图①,设 AB' 与 BC 的交点为 O,$\because \angle BAC=120^\circ$,$AB=AC$,$\therefore \angle B=\angle C=30^\circ$. 由折叠的性质可知 $\angle B'=\angle B=30^\circ$,$\therefore \angle DOB'=\angle B'DO=60^\circ$,$\therefore \angle DOB'=90^\circ$,$\therefore DO=\frac{1}{2}B'D=\frac{1}{2}BD$,$\therefore BO=BD+DO=BD+\frac{1}{2}BD=\frac{3}{2}BD$. $\because$ 在 Rt$\triangle ABO$ 中,$BO=AB\cdot\cos 30^\circ=\frac{3}{2}BD$,$\therefore \frac{3}{2}BD=2\sqrt{3}$,$\therefore BD=\frac{4\sqrt{3}}{3}$;②当点 B' 在 BC 的上方时,如解图②,由折叠得 $\angle ADB'=\angle ADB=\frac{1}{2}\angle BDB'=60^\circ$,$\therefore \angle B=30^\circ$,$\therefore \angle BAD=90^\circ$,$\therefore AB=4\times\frac{\sqrt{3}}{3}=\frac{4\sqrt{3}}{3}$. 综上所述,$BD$ 的长为 $\frac{4\sqrt{3}}{3}$或$\frac{8\sqrt{3}}{3}$.

图① 图②

第 15 题解图

视频讲解 白卷·15题

更多新考法试题 见《重难题新考法》P25 重难题二

参解题

三、解答题(本大题共 8 个小题,共 75 分)

16. 解:(1)原式 $=1+4+2-\sqrt{7}=7-\sqrt{7}$ ……3 分

(2) 原式 $=4x^2-4-(4x^2-4x+1)=4x^2-4-4x^2+4x-1=4x-5$ ……5 分

17. 解:(1)40,78.5;……4 分

【解法提示】对 A 款 AI 机器人评分抽取的样本容量为 $6+6+4+4=20$,$\therefore$ 本次抽取的问卷共有 $20\div 40\%=50$(份),$\because$ 对 A 款 AI 机器人评分的中位数为第 10 和 11 个数据的平均数,$\therefore$ 将 $70\leqslant x<80$ 这一组的评分按从小到大的顺序排列为:74,75,78,78,79,79,$\therefore$ 第 10 和 11 个数据分别为 78,79,$\therefore$ 中位数为 $\frac{1}{2}\times(78+79)=78.5$ 分.

(2)由(1)得对 A 款 AI 机器人评分的中位数为 78.5 分,$\therefore$ 78.5 分<80 分,$\therefore$ 对 A 款 AI 机器人感到满意的人数未超过一半;……6 分

(3)由条形统计图得,对 B 款 AI 机器人评分为非常满意的有 2 人,$\therefore 300\times\frac{2}{20}=30$(人),

答:估计此次问卷调查活动中对 B 款 AI 机器人非

第二步:结合菱形的性质和图②中的已知条件进行求解.

<pFig>第10题解图</pFig><quad>(204,50),(325,111)</quad>

二、填空题(每小题3分,共15分)

11.$ x\geq - 1 $且$ x\ne 0 $

12.0【解析】由题意得,反比例函数$ y=\frac{1+2m}{x} $的图象位于第一、三象限,$ \therefore 1+2m>0,\therefore m>-\frac{1}{2},\therefore m $的最小整数值为0.

13.$ \frac{2}{9} $【解析】根据题意,画树状图如解图,

<pFig>第13题解图</pFig><quad>(145,291),(388,357)</quad>

由树状图知,共有9种等可能的结果,其中可以呈现青色的结果有2种,$ \therefore P(\text{可以呈现青色})=\frac{2}{9} $.

14.$ 2\sqrt{10}+\frac{\sqrt{10}}{2}\pi $ 【解析】如解图,连接OB,AC,由题意可知
$ OA=OB=OC=\sqrt{3^{2}+1^{2}}=\sqrt{10},AC=\sqrt{2^{2}+4^{2}}=2\sqrt{5},\therefore OA^{2}+OC^{2}=AC^{2},\therefore\angle AOC=90^{\circ},\therefore $圆心角AOC所对的弧长为$ \frac{90\times\pi\times\sqrt{10}}{180}=\frac{\sqrt{10}}{2}\pi,\therefore $扇形AOC的周长为$ 2\sqrt{10}+\frac{\sqrt{10}}{2}\pi $.

<pFig>第14题解图</pFig><quad>(362,436),(461,510)</quad>

知识精准回顾:$ n^{\circ} $的圆心角所对的弧长计算公式为$l=\frac{n\pi r}{180} $.

15.$ \frac{4\sqrt{3}}{3} $或$ \frac{8\sqrt{3}}{3} $ 【解析】当$ \angle BDB^{\prime}=120^{\circ} $时,分两种情况:①当点B'在BC的下方时,如解图①,设AB'与BC的交点为O,$ \because\angle BAC = 120^{\circ},AB = AC,\therefore\angle B=\angle C=30^{\circ} $.由折叠的性质可知
$ \angle B^{\prime}=\angle B=30^{\circ},\because\angle BDB^{\prime}=120^{\circ},\therefore\angle B^{\prime}DO=60^{\circ},\therefore\angle DOB^{\prime}=90^{\circ},\therefore DO=\frac{1}{2}B^{\prime}D=\frac{1}{2}BD,\therefore BO=BD+DO=BD+\frac{1}{2}BD=\frac{3}{2}BD.\because $在Rt$\triangle ABO $中,$ BO=AB\cdot\cos30^{\circ}=\frac{3}{2}BD,\therefore\frac{3}{2}BD=2\sqrt{3},\therefore BD=\frac{4\sqrt{3}}{3} $;②当点B'在BC的上方时,如解图②,由折叠得$ \angle ADB^{\prime}=\angle ADB=\frac{1}{2}\angle BDB^{\prime}=60^{\circ},\because\angle B=30^{\circ},\therefore\angle BAD=90^{\circ},\because AB=4,\therefore BD=\frac{AB}{\cos30^{\circ}}=\frac{4}{\frac{\sqrt{3}}{2}}=\frac{8\sqrt{3}}{3} $.综上所述,BD的长为$ \frac{4\sqrt{3}}{3} $或$ \frac{8\sqrt{3}}{3} $.

<pFig>第15题解图</pFig><quad>(516,188),(809,266)</quad>

<pFig>视频讲解\n白卷·15题</pFig><quad>(639,289),(713,350)</quad>

$ \underline{\text{更多新考法实体 见《重难题新考法》P25重难题二}} $

$ \underline{\text{多解题}} $

三、解答题(本大题共8个小题,共75分)

16.解:(1)原式=1+4+2-\sqrt{7}=7-\sqrt{7}$ ……3分
$ =7;……5分

(2)原式$ =4x^{2}-4-(4x^{2}-4x+1) $
$ =4x^{2}-4-4x^{2}+4x-1 $……3分
$ =4x-5 $.……5分

17.解:(1)40,78.5;……4分

【解法提示】$ \because $对A款AI机器人评分抽取的样本容量为$6+6+4+4=20,$ \therefore $本次抽取的问卷共有20÷20=40(份).$ \because $对A款AI机器人评分的中位数为第10和11个数据的平均数,$ \therefore $将$ 70\leq x < 80 $这一组的评分按从小到大的顺序排列为:74,75,78,78,79,79,$ \therefore $第10和11个数据分别为78,79,$ \therefore $中位数为$ \frac{1}{2}\times(78 + 79)=78.5 $分.

(2)由(1)得对A款AI机器人评分的中位数为78.5分,
$ \because $78.5分< 80分,
$ \therefore $对A款AI机器人感到满意的人数未超过一半;……6分

(3)由条形统计图得,对B款AI机器人评分为非常满意的有2人,
$ \therefore 300\times\frac{2}{20}=30 $(人),

答:估计此次问卷调查活动中对B款AI机器人非

Figure 2. Representative parsing results (I).

高一2407班下学期课表（2025年2月17日执行）

时间	节次	星期一	星期二	星期三	星期四	星期五	星期六	星期日
7:00	到班							07:50到班
07:00--07:20	晨读		英语	语文	英语	语文	语文	
07:20--07:50	早自习	英语/升旗	语文	英语	语文	英语	英语	
08:00--08:40	1	语文	英语	数学	英语	语文	英语	辅优
08:50--09:30	2	英语	数学	数学	英语	英语	英语	
09:30--10:00	大课间活动							
10:00--10:40	3	物理	物理	语文	数学	数学	自习	
10:40--10:50	眼保健操							
10:50--11:30	4	历史	语文	英语	语文	生物	语文	
11:40--12:20	5	数学	语文	阅读	物理	物理	语文	
12:20--13:05	午餐+打扫卫生							
13:05--13:20	中/英文练字							
13:20--14:00	午休							
14:10--14:50	6	生物	自习	化学	地理	体育	生物	化学
15:00--15:40	7	信息	生物	地理	美术	音乐	生物	化学
15:50--16:30	8	化学	化学	体育	历史	化学	数学	物理
16:40--17:20	9	心理单/校本双	听力	生物	劳动	听力	数学	物理
17:20--17:50	晚餐							晚餐
17:50--18:10	活动+打扫卫生							活动
18:10--18:50	晚提前							换座位
19:00--19:45	晚一	生物	物理	生物	物理	数学	休	班会
19:45--19:50	眼保健操							眼保健操
20:00--20:45	晚二	数学	化学	数学	化学			自习
20:55--21:40	晚三		数学自习		数学自习		息	
21:40--21:45	放学							
22:30	熄灯睡觉							

辅优

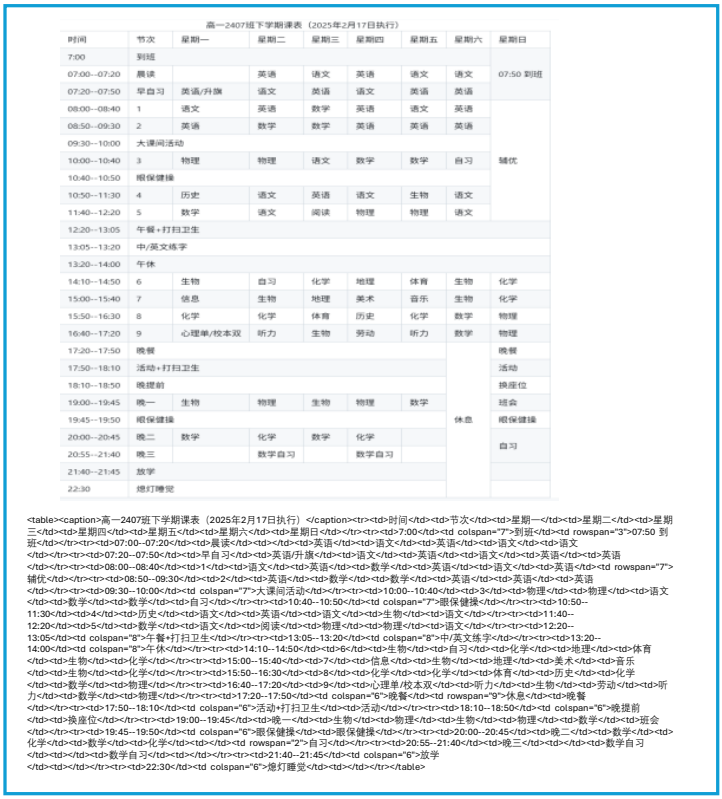

高一2407班下学期课表（2025年2月17日执行）

时间	节次	星期一	星期二	星期三	星期四	星期五	星期六	星期日
7:00	到班							
07:00--07:20	晨读		英语	语文	英语	语文	语文	07:50 到班
07:20--07:50	早自习	英语/升旗	语文	英语	语文	英语	英语	
08:00--08:40	1	语文	英语	数学	英语	语文	英语	
08:50--09:30	2	英语	数学	数学	英语	英语	英语	
09:30--10:00	大课间活动							
10:00--10:40	3	物理	物理	语文	数学	数学	自习	辅优
10:40--10:50	眼保健操							
10:50--11:30	4	历史	语文	英语	语文	生物	语文	
11:40--12:20	5	数学	语文	阅读	物理	物理	语文	
12:20--13:05	午餐+打扫卫生							
13:05--13:20	中/英文练字							
13:20--14:00	午休							
14:10--14:50	6	生物	自习	化学	地理	体育	生物	化学
15:00--15:40	7	信息	生物	地理	美术	音乐	生物	化学
15:50--16:30	8	化学	化学	体育	历史	化学	数学	物理
16:40--17:20	9	心理单/校本双	听力	生物	劳动	听力	数学	物理
17:20--17:50	晚餐							晚餐
17:50--18:10	活动+打扫卫生							活动
18:10--18:50	晚提前							换座位
19:00--19:45	晚一	生物	物理	生物	物理	数学	休息	班会
19:45--19:50	眼保健操							眼保健操
20:00--20:45	晚二	数学	化学	数学	化学			自习
20:55--21:40	晚三		数学自习		数学自习			
21:40--21:45	放学							
22:30	熄灯睡觉							

<table><caption>高一2407班下学期课表（2025年2月17日执行）</caption><tr><td>时间</td><td>节次</td><td>星期一</td><td>星期二</td><td>星期三</td><td>星期四</td><td>星期五</td><td>星期六</td><td>星期日</td></tr><tr><td>7:00</td><td colspan="7">到班</td></tr><tr><td>07:00--07:20</td><td>晨读</td><td></td><td>英语</td><td>语文</td><td>英语</td><td>语文</td><td>语文</td><td rowspan="3">07:50 到班</td></tr><tr><td>07:20--07:50</td><td>早自习</td><td>英语/升旗</td><td>语文</td><td>英语</td><td>语文</td><td>英语</td><td>英语</td></tr><tr><td>08:00--08:40</td><td>1</td><td>语文</td><td>英语</td><td>数学</td><td>英语</td><td>语文</td><td>英语</td><td rowspan="7">辅优</td></tr><tr><td>08:50--09:30</td><td>2</td><td>英语</td><td>数学</td><td>数学</td><td>英语</td><td>英语</td><td>英语</td></tr><tr><td>09:30--10:00</td><td colspan="7">大课间活动</td></tr><tr><td>10:00--10:40</td><td>3</td><td>物理</td><td>物理</td><td>语文</td><td>数学</td><td>数学</td><td>自习</td></tr><tr><td>10:40--10:50</td><td colspan="7">眼保健操</td></tr><tr><td>10:50--11:30</td><td>4</td><td>历史</td><td>语文</td><td>英语</td><td>语文</td><td>生物</td><td>语文</td></tr><tr><td>11:40--12:20</td><td>5</td><td>数学</td><td>语文</td><td>阅读</td><td>物理</td><td>物理</td><td>语文</td></tr><tr><td>12:20--13:05</td><td colspan="8">午餐+打扫卫生</td></tr><tr><td>13:05--13:20</td><td colspan="8">中/英文练字</td></tr><tr><td>13:20--14:00</td><td colspan="8">午休</td></tr><tr><td>14:10--14:50</td><td>6</td><td>生物</td><td>自习</td><td>化学</td><td>地理</td><td>体育</td><td>生物</td><td>化学</td></tr><tr><td>15:00--15:40</td><td>7</td><td>信息</td><td>生物</td><td>地理</td><td>美术</td><td>音乐</td><td>生物</td><td>化学</td></tr><tr><td>15:50--16:30</td><td>8</td><td>化学</td><td>化学</td><td>体育</td><td>历史</td><td>化学</td><td>数学</td><td>物理</td></tr><tr><td>16:40--17:20</td><td>9</td><td>心理单/校本双</td><td>听力</td><td>生物</td><td>劳动</td><td>听力</td><td>数学</td><td>物理</td></tr><tr><td>17:20--17:50</td><td colspan="7">晚餐</td><td>晚餐</td></tr><tr><td>17:50--18:10</td><td colspan="7">活动+打扫卫生</td><td>活动</td></tr><tr><td>18:10--18:50</td><td colspan="7">晚提前</td><td>换座位</td></tr><tr><td>19:00--19:45</td><td>晚一</td><td>生物</td><td>物理</td><td>生物</td><td>物理</td><td>数学</td><td rowspan="3">休息</td><td>班会</td></tr><tr><td>19:45--19:50</td><td colspan="7">眼保健操</td><td>眼保健操</td></tr><tr><td>20:00--20:45</td><td>晚二</td><td>数学</td><td>化学</td><td>数学</td><td>化学</td><td></td><td rowspan="2">自习</td></tr><tr><td>20:55--21:40</td><td>晚三</td><td></td><td>数学自习</td><td></td><td>数学自习</td><td></td></tr><tr><td>21:40--21:45</td><td colspan="7">放学</td></tr><tr><td>22:30</td><td colspan="6">熄灯睡觉</td></tr></table>

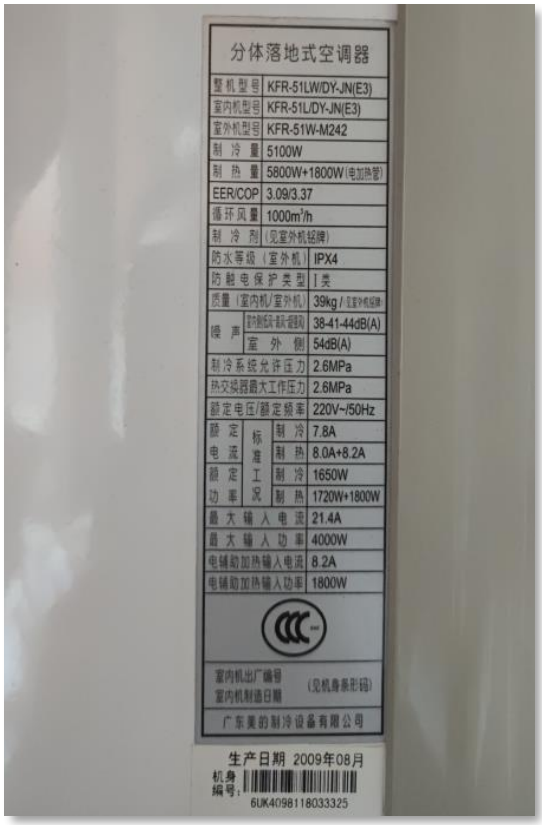

分体落地式空调器

整机型号	KFR-51LW/DY-JN(E3)
室内机型号	KFR-51L/DY-JN(E3)
室外机型号	KFR-51W-M242
制冷量	5100W
制热量	5800W+1800W(电加热管)
EER/COP	3.09/3.37
循环风量	1000m³/h
制冷剂	(见室外机铭牌)
防水等级（室外机）	IPX4
防触电保护类型	I类
质量（室内机/室外机）	39kg/（见室外机铭牌）
噪声 室内侧(低风-高风-超强风)	38-41-44dB(A)
噪声 室外侧	54dB(A)
制冷系统允许压力	2.6MPa
热交换器最大工作压力	2.6MPa
额定电压/额定频率	220V~/50Hz
额定电流 标准工况 制冷	7.8A
额定电流 标准工况 制热	8.0A+8.2A
额定功率 标准工况 制冷	1650W
额定功率 标准工况 制热	1720W+1800W
最大输入电流	21.4A
最大输入功率	4000W
电辅助加热输入电流	8.2A
电辅助加热输入功率	1800W

室内机出厂编号
室内机制造日期 （见机身条形码）
广东美的制冷设备有限公司

生产日期 2009年08月
机身编号：6UK4098118033325

分体落地式空调器			
整机型号	KFR-51LW/DY-JN(E3)		
室内机型号	KFR-51L/DY-JN(E3)		
室外机型号	KFR-51W-M242		
制冷量	5100W		
制热量	5800W+1800W(电加热管)		
EER/COP	3.09/3.37		
循环风量	$ 1000m^{3}/h $		
制冷剂	(见室外机铭牌)		
防水等级(室外机)	IPX4		
防触电保护类型	I类		
质量(室内机/室外机)	39kg/(见室外机铭牌)		
噪声	室内侧(低风-高风-超强风)	38-41-44dB(A)	
	室外侧	54dB(A)	
制冷系统允许压力	2.6MPa		
热交换器最大工作压力	2.6MPa		
额定电压/额定频率	220V~/50Hz		
额定电流	标准工况	制冷	7.8A
		制热	8.0A+8.2A
额定功率	标准工况	制冷	1650W
		制热	1720W+1800W
最大输入电流	21.4A		
最大输入功率	4000W		
电辅助加热输入电流	8.2A		
电辅助加热输入功率	1800W		
图1(483,728),(608,800)			
室内机出厂编号 室内机制造日期 (见机身条形码)			
广东美的制冷设备有限公司			

<table><caption></caption><tr><td colspan="5">分体落地式空调器</td></tr><tr><td colspan="2">整机型号</td><td colspan="3">KFR-51LW/DY-JN(E3)</td></tr><tr><td colspan="2">室内机型号</td><td colspan="3">KFR-51L/DY-JN(E3)</td></tr><tr><td colspan="2">室外机型号</td><td colspan="3">KFR-51W-M242</td></tr><tr><td colspan="2">制冷量</td><td colspan="3">5100W</td></tr><tr><td colspan="2">制热量</td><td colspan="3">5800W+1800W(电加热管)</td></tr><tr><td colspan="2">EER/COP</td><td colspan="3">3.09/3.37</td></tr><tr><td colspan="2">循环风量</td><td colspan="3">$ 1000m^{3}/h $</td></tr><tr><td colspan="2">制冷剂</td><td colspan="3">(见室外机铭牌)</td></tr><tr><td colspan="2">防水等级(室外机)</td><td colspan="3">IPX4</td></tr><tr><td colspan="2">防触电保护类型</td><td colspan="3">I类</td></tr><tr><td colspan="2">质量(室内机/室外机)</td><td colspan="3">39kg/(见室外机铭牌)</td></tr><tr><td rowspan="2">噪声</td><td>室内侧(低风-高风-超强风)</td><td>38-41-44dB(A)</td></tr><tr><td>室外侧</td><td>54dB(A)</td></tr><tr><td colspan="2">制冷系统允许压力</td><td colspan="3">2.6MPa</td></tr><tr><td colspan="2">热交换器最大工作压力</td><td colspan="3">2.6MPa</td></tr><tr><td colspan="2">额定电压/额定频率</td><td colspan="3">220V~/50Hz</td></tr><tr><td rowspan="2">额定电流</td><td rowspan="2">标准工况</td><td>制冷</td><td>7.8A</td></tr><tr><td>制热</td><td>8.0A+8.2A</td></tr><tr><td rowspan="2">额定功率</td><td rowspan="2">标准工况</td><td>制冷</td><td>1650W</td></tr><tr><td>制热</td><td>1720W+1800W</td></tr><tr><td colspan="2">最大输入电流</td><td colspan="3">21.4A</td></tr><tr><td colspan="2">最大输入功率</td><td colspan="3">4000W</td></tr><tr><td colspan="2">电辅助加热输入电流</td><td colspan="3">8.2A</td></tr><tr><td colspan="2">电辅助加热输入功率</td><td colspan="3">1800W</td></tr><tr><td colspan="5">图1(483,728),(608,800)</td></tr><tr><td colspan="5">室内机出厂编号
室内机制造日期
(见机身条形码)</td></tr><tr><td colspan="5">广东美的制冷设备有限公司</td></tr></table>

生产日期 2009年08月

机身编号：<pFig>图2</pFig><quad>(452,938),(664,966)</quad>6UK4098118033325

Figure 3. Representative parsing results (II).

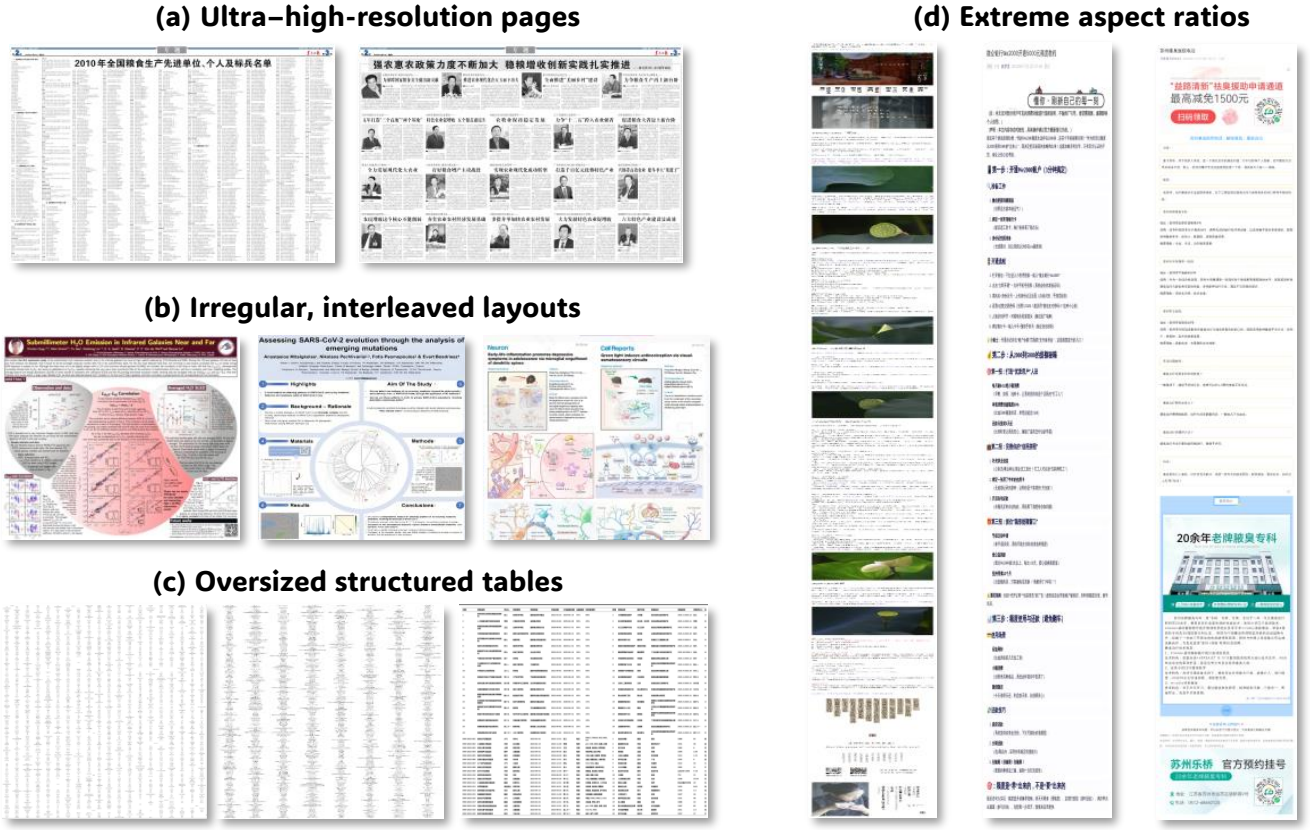

Figure 4. **Error Case Taxonomy and Examples.** Web-sourced documents where *DocHumming* reaches the 8,192-token cap and exhibits repetition: (a) ultra-high-resolution pages, (b) irregular/interleaved layouts, (c) oversized structured tables, and (d) extreme aspect ratios.